Biosensors and Bioelectronics 26 (2011) 3181–3186

Contents lists available at ScienceDirect

Biosensors and Bioelectronics

journal homepage: www.elsevier.com/locate/bios

Disposable biosensor based on graphene oxide conjugated with tyrosinase assembled gold nanoparticles

Wei Song[a,b], Da-Wei Li[a], Yuan-Ting Li[a], Yang Li[a], Yi-Tao Long[a,*]

[a] Shanghai Key Laboratory of Functional Materials Chemistry & Department of Chemistry, East China University of Science and Technology, 130 Meilong Road Shanghai 200237, China
[b] Department of Applied Chemistry, Nanjing College of Chemical and Technology, 625 Geguan Road Nanjing 210048, China

ARTICLE INFO

Article history:
Received 20 August 2010
Received in revised form
28 November 2010
Accepted 13 December 2010
Available online 30 December 2010

Keywords:
Graphene oxide
Gold nanoparticles
Tyrosinase
Screen printed electrode
Disposable biosensor

ABSTRACT

A highly efficient enzyme-based screen printed electrode (SPE) was obtained by using covalent attachment between 1-pyrenebutanoic acid, succinimidyl ester (PASE) adsorbing on the graphene oxide (GO) sheets and amines of tyrosinase-protected gold nanoparticles (Tyr–Au). Herein, the bi-functional molecule PASE was assembled onto GO sheets. Subsequently, the Tyr–Au was immobilized on the PASE–GO sheets forming a biocompatible nanocomposite, which was further coated onto the working electrode surface of the SPE. The characterization of obtained nanocomposite and modified SPE surface was investigated by atomic force microscopy (AFM), transmission electron microscopy (TEM) and scanning electron microscopy (SEM). Attributing to the synergistic effect of GO–Au integration and the good biocompatibility of the hybrid-material, the fabricated disposable biosensor (Tyr–Au/PASE–GO/SPE) exhibited a rapid amperometric response (less than 6 s) with a high sensitivity and good storage stability for monitoring catechol. This method shows a good linearity in the range from 8.3×10^{-8} to 2.3×10^{-5} M for catechol with a squared correlation coefficient of 0.9980, a quantitation limit of 8.2×10^{-8} M ($S/N = 10$) and a detection limit of 2.4×10^{-8} M ($S/N = 3$). The Michaelis–Menten constant was measured to be 0.027 mM. This disposable tyrosinase biosensor could offer a great potential for rapid, cost-effective and on-field analysis of phenolic compounds.

1. Introduction

Phenolic compounds have been become a group of considerable contaminants in medical, food, ground and surface waters. The determination of phenolic compounds is of great importance to the protection of public health and the environment (Shan et al., 2007). Among electrochemical methods, amperometric biosensors based on tyrosinase (Tyr) and polyphenol oxidase (PPO) have proved to be sensitive and convenient for the determination of phenolic compounds (Liu et al., 2005). To achieve the construction quality of Tyr biosensor, the signal amplification and the stable immobilization of the enzyme on the electrode surface are of considerable interest (Kotte et al., 1995). More recently, various supporting materials have been successfully utilized to immobilize Tyr on the electrode (Arecchi et al., 2010; Portaccio et al., 2010; Tan et al., 2009, 2010; Wang et al., 2008; Zhao et al., 2009). In addition, there are several works related to the fabrication of tyrosinase biosensors immobilized on the screen printed electrode (SPE) (Chang et al., 2002; Montereali et al., 2010; Sapelnikova et al., 2003; Solná et al., 2005), which can be incorporated in portable systems as an alterative detection method for the direct on-site analysis (Kampouris et al., 2009).

In the past years, graphene-oriented electrochemistry, bioelectrochemistry as well as electrocatalysis have greatly stimulated research interests (Chen et al., 2010). Graphene, with an atomically thin two-dimensional lattice of sp^2 carbon atoms, has emerged in recent years as a novel class of nano-material, with remarkable electronic and mechanical properties (Sun et al., 2008). The excellent electrochemical behaviors of graphene indicate graphene is a promising electrode material in electroanalysis (Shao et al., 2010). Graphene oxide (GO), bearing oxygen functional groups on its basal planes and edges, is a single sheet of GO and exhibits a good performance (Wang et al., 2010). The solubility of GO in water and other solvents allows it to be uniformly deposited onto the wide ranging substrates in the form of thin films or networks which makes it potentially useful for macro-electronics (Mkhoyan et al., 2009). Individual GO sheet has an atomically flat surface, and can serve as an ideal solid substrate for enzyme immobilization (Zhang et al., 2010a). Because of their interesting electrochemical behaviors, GO nanomaterials have been well studied for enzyme immobilization and biosensor applications (Liu et al., 2010; Wang et al., 2009; Zhou et al., 2010a,b; Zuo et al., 2010). In these studies, enzyme was immo-

* Corresponding author. Tel.: +86 21 642 50032; fax: +86 21 642 50032.
E-mail address: ytlong@ecust.edu.cn (Y.-T. Long).

0956-5663/$ – see front matter © 2010 Elsevier B.V. All rights reserved.
doi:10.1016/j.bios.2010.12.022

bilized on the GO sheets through physical adsorption, electrostatic interaction and covalent attachment.

The integration of nanomaterials on gold nanoparticles (AuNPs) potentially paves a new way to enhance their electronic, chemical, and electrochemical properties (Fang et al., 2010). Due to their unique chemical and physical properties, AuNPs have been used widely in the fabrication of biosensors. Especially, the unique properties of AuNPs provide a suitable microenvironment for biomolecules immobilization and facilitate electron transfer (Shan et al., 2010). Recently, graphene–AuNPs composites have been well prepared and used as the electro-catalysts for biosensing glucose, oxygen, and uric acid (Hong et al., 2010; Li et al., 2009; Lu et al., 2008; Zhou et al., 2010a).

Compared with the covalent functionalization, some of the simple and versatile noncovalent methods through supermolecular interactions such as π–π stacking (Xu et al., 2008) have the advantage of preserving the unique electronic properties of GO without serious damage. Through this manner, GO can be functionalized with the designed properties when it combined with the planar aromatic molecules (Zhang et al., 2010b). Herein, we applied 1-pyrenebutanoic acid, succinimidyl ester (PASE) as the noncovalent functionalization reagent adsorbing onto the GO sheet via π–π interaction (Subrahmanyam et al., 2009). PASE could react with carbon nanotubes (CNTs) by π-stacking, resulting in a stable composite nanomaterial. Then, the protein could covalently bind with PASE-functionalized CNTs by forming amide bond (Chen et al., 2001). According to the same method as above, Tyr can be assembled onto the PASE-functionalized GO sheets with a high degree of control and specificity. The protein-protected AuNPs and AgNPs have been well studied for the fabrication of CNTs/metal nanoparticles hybrid. These researches indicate that it is possible to fabricate structure-controllable CNTs–AuNPs hybrids and explore the potential application of these nanomaterials in the field of biosensering (Bale et al., 2007; Kurppa et al., 2007; Wei et al., 2010). In our study, Tyr-protected AuNPs (Tyr–Au) was immobilized onto the GO sheets by using PASE as a linkage reagent. Subsequently, the Tyr–Au/PASE–GO nanocomposite was modified on the surface of working electrode of the SPE, fabricating a new disposable tyrosinase biosensor. The procedure of fabricating the Tyr–Au/PASE–GO/SPE is illustrated in Scheme 1. The morphologies of the nanocomposite were characterized by atomic force microscopy (AFM), scanning electron microscopy (SEM) and transmission electron microscopy (TEM). The proposed biosensor exhibits fast and sensitive amperometric responses to catechol. The optimized parameters such as working potential, pH of supporting electrolyte were studied. The amperometric response of the proposed biosensor to catechol concentration has been investigated and the kinetic parameter was calculated. The results showed that the developed biosensor (Tyr–Au/PASE–GO/SPE) exhibited good stability and high sensitivity for the determination of catechol, showing a promising performance as a preliminary application in environmental monitoring.

2. Materials and methods

2.1. Reagents and materials

All reagents were of analytical grade and were used as received without further purification. Tyrosinase (EC 1.14.18.1, 3900 U mg^{-1} from mushroom) was bought from Sigma–Aldrich (USA). N,N'-Dicyclohexyl carbodiimide (DCC), 1-Pyrenebutylacid and N-hydroxysuccinimide were obtained from Aladdin (Shanghai, China). $HAuCl_4$ and $NaBH_4$ and other reagents were purchased from Sinopharm Chemical Reagent Co., Ltd. (Shanghai, China). Graphite powder (99.9995%, 325 mesh) was purchased from Alfa Aesar (Ward Hill, MA, USA). The supporting electrolyte was 0.1 M phosphate buffer solution (PBS) prepared with Na_2HPO_4 and KH_2PO_4, and the pH was adjusted with NaOH or H_3PO_4. Deionized water obtained with a Milli-Q System (Billerica, MA, USA) was used for preparing all solutions.

2.2. Instruments

The UV–vis absorption spectra were collected using the USB2000+ spectrometer with an Ocean Optics DT-mini-2 halogen recourse (Ocean Optics, USA). Fourier transform infrared spectroscopy (FTIR) was recorded on a Nicolet Avatar 360 spectrometer (Thermo, USA). Atomic force microscopic (AFM) study was performed with NanoScope IIIa (Veeco, USA) operating in the tapping mode. Scanning electron microscopy (SEM) images were obtained using a JSM-6360LV scanning electron microscope (JEOL Ltd., Japan). Transmission electron microscopy (TEM) image was taken by a JEOL 3010 electron microscope (JEOL Ltd., Japan). All electrochemistry experiments were performed on a CHI 1232A portable electrochemical analyzer (Chenhua, Shanghai, China). According to our previous work (Song et al., 2010), the screen printed electrode was produced on an AT-25P machine (ATMACHAMP ENT. Corp., Taiwan) using polyester screens with appropriate stencil designs.

2.3. Preparation of Tyr–Au/PASE–GO modified SPE

PASE was synthesized according to the method described by the previous report (Wu, 2008). In brief, a solution of DCC (43 mg) in dry THF (2 mL) was added drop-wise to the stirred reaction mixture of 1-pyrenebutyl acid (600 mg) and N-hydroxysuccinimide (24 mg) in THF (5 mL) at 0 °C under argon. After stirring overnight at room temperature, the resulting mixture was filtered. The solvent was removed under reduced pressure to give the compound PASE as a yellow solid, which was purified by recrystallization from ethanol.

Graphene oxide (0.2 mg mL^{-1}) was prepared from graphite powder according to the modified Hummers method (Kovtyukhova et al., 1999). PASE–GO was prepared according to the literature (Yang et al., 2008). 2 mg mL^{-1} PASE solution in DMF was mixed with the same volume of GO for 2 h while stirring. Subsequently, the mixture was centrifuged at 12,000 rpm for 10 min to remove the supernatant. The resulting PASE–GO composite was then dispersed in 1 mL 0.02 M pH 7.0 PBS solution.

Tyr–Au was prepared following a previously described procedure (Wei et al., 2010). Briefly, 2 mL of 1 mM $HAuCl_4$ aqueous solution was mixed with 200 μL of Tyrosinase solution (5 mg mL^{-1}) in 0.02 M pH 7.0 PBS under vigorous stirring. Ten minutes later, freshly prepared $NaBH_4$ aqueous solution (1%) was added to the mixed solution drop-wise until the color of the AuNPs did not change.

1 mL of Tyr–Au solution was mixed with 1 mL of PASE–GO solution. Then the mixture was kept at 4 °C for 18 h with occasional shaking. After centrifugation at 12,000 rpm for 20 min, the Tyr–Au/PASE–GO nanocomposite was washed with 0.02 M pH 7.0 PBS. This stock was stored under refrigeration (4 °C) before use.

The SPE was pretreated in 0.1 M PBS (pH 7.0) containing 0.1 M KCl by applying an anodic potential of 1.7 V for 3 min before use. Prior to the modification, the SPE was washed with water several times. Then 5 μL of Tyr–Au/PASE–GO solution was dropped onto the working electrode area. After dried at 4 °C, the modified SPE was rinsed with water three times. And the Tyr–Au/PASE–GO modified SPE was obtained. The dried electrode was kept in 0.02 M pH 7.0 PBS under refrigeration when not in use. For the comparison, Tyr/SPE and Tyr/PASE–GO/SPE were also fabricated.

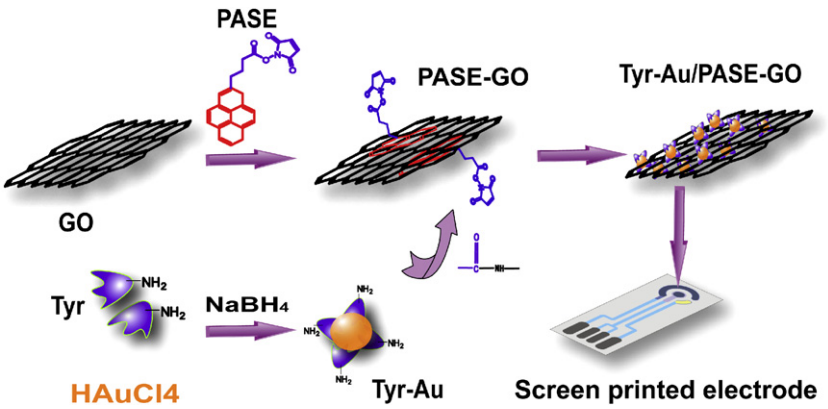

Scheme 1. Assembling process of Tyr–Au/PASE–GO on SPE.

2.4. Electrochemical measurements

Voltammetric and amperometric measurements were carried out with a CHI 1232A portable electrochemical analyzer. The modified circular area (2 mm in diameter) was used as a working electrode. The reference electrode was printed with 40% silver chloride in silver paste, and the auxiliary electrode was printed with carbon ink. Cyclic voltammetric measurements were performed in PBS at a scan rate of 50 mV s^{-1}. Amperometric measurements were performed in a 10 mL electrochemical cell under magnetically stirring. All experiments were carried out at room temperature in 0.1 M PBS containing 0.1 M KCl.

3. Results and discussion

3.1. Non-covalent functionalization of GO with PASE

Similar to CNTs, noncovalent functionalization of GO was performed by mixing GO with PASE, which is a bi-functional molecule with pyrenyl group at one end and N-hydroxysuccinimide (NHS) group at another end. PASE can irreversibly adsorb onto the GO in DMF through noncovalent interaction. The pyrenyl group, being highly aromatic in nature, is known to interact strongly with the basal plane of graphite via π-stacking (Jaegfeldt et al., 1983), providing a fixation point for PASE on the GO. And the succinimidyl ester group is highly reactive to the nucleophilic substitution by amines that existed in abundance on the surface of tyrosinase, resulting in the formation of an amide bond. Through this manner, tyrosinase was immobilized on the GO sheets with a high efficiency. Fig. 1 shows the AFM image of PASE functional GO sheets. The sample used for AFM study was prepared by depositing the corresponding dispersion on the silicon wafer dried under vacuum at room temperature. The mean thickness of single PASE–GO sheet was measured to be about 2.9 nm, which is almost triple the thickness of pure GO sheet (about 1 nm) reported by pervious work (Niyogi et al., 2006). Thus, we consumed that PASE molecules have covered both sides of GO sheets.

UV–vis spectra and FT-IR spectra were used to investigate the structural modification of GO and identify the successful functionalization of GO with PASE (Fig. 2). Fig. 2A illustrates the UV–vis absorption spectrum of PASE and PASE–GO. As it can be seen, the main absorption peaks of the PASE–GO appear at 283, 335 and 354 nm, respectively, which are red shifted by 7 nm in comparison with that of the pure PASE. This is mainly due to the π–π interaction between the GO sheets and the large aromatic ring of PASE. As shown in Fig. 2B, the FT-IR spectra of PASE–GO shows the absorption bands at 3037, 2932, 2874, 1812, 1785, 1728, 1376, 1213, 1066, 840 and 663 cm^{-1}, which are contributed to the characteristic absorption peaks of PASE. These peaks are similar to the resulting FT-IR spectra of pure PASE, suggesting that PASE was successfully assembled onto GO sheets by π-stacking interaction.

3.2. Characterization of Tyr–Au/PASE–GO modified SPE

The morphology of the Tyr–Au/PASE–GO nanocomposite is examined by TEM observation. Figure S1 (in supplementary materials) shows the TEM image of the obtained GO sheets, illustrating the flake-like shapes of graphene. It is clear that AuNPs distributed well on GO sheets, evidencing the well-behaved assembly process. The morphological character of the Tyr–Au/PASE–GO modified SPE is investigated by using SEM (Fig. 3). Compared to the SEM image of bare SPE (Fig. 3A), it is found that the Tyr–Au/PASE–GO biocomposite film on the working electrode exhibited a porous surface with three-dimensional (3D) network (Fig. 3B). As it can be seen, the nanocomposite deposited on the surface of the electrode is intertwined with each other into a complex 3D architecture. The Tyr molecule has acted as a glue reagent connecting the PASE–GO with AuNPs. Such morphological characteristics might result in high loading of enzyme and fast response to the substrate.

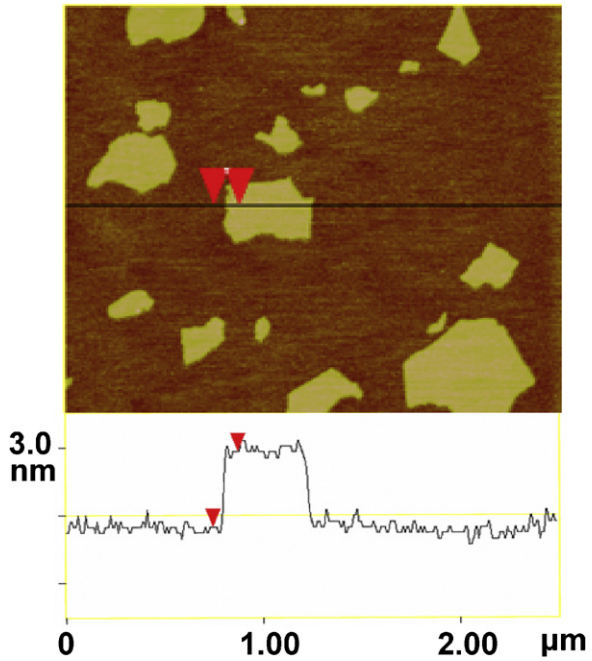

Fig. 1. Tapping-mode AFM image of PASE–GO and the height profile along the dashed line in the panel.

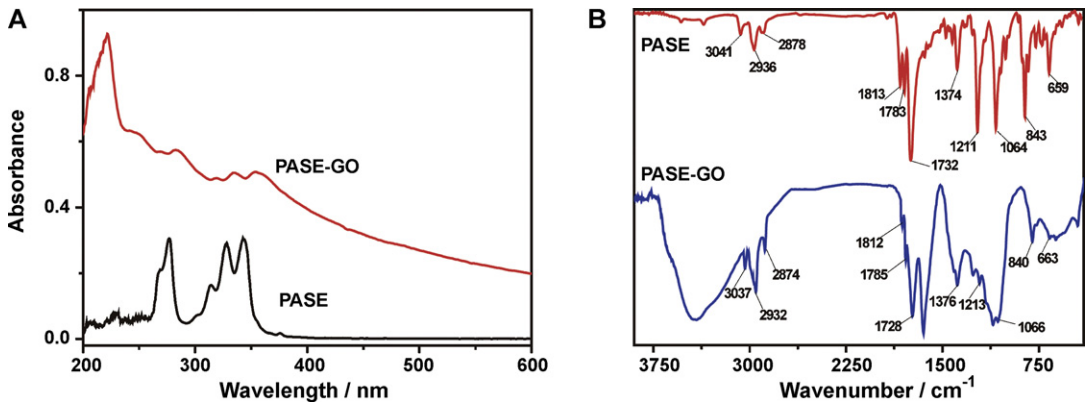

Fig. 2. UV–vis spectra (A) and FT-IR spectra (B) of GO and PASE–GO.

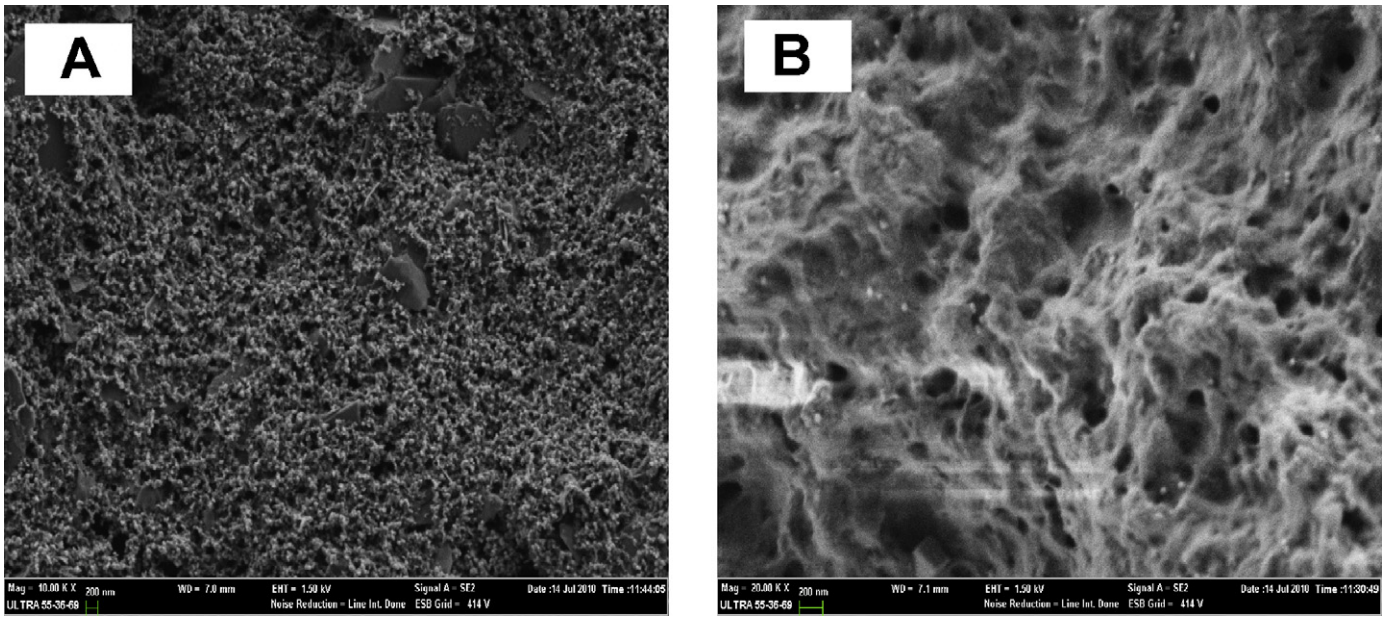

Fig. 3. SEM images of (A) bare SPE and (B) Tyr–Au/PASE–GO modified SPE.

3.3. CV curves for catechol at the SPE

In this paper, catechol was used as the typical model of phenolic compounds to study the electrochemical sensing characteristics of the disposable Tyr–Au/PASE–GO nanobiocomposite biosensor. Tyrosinase can exist as monophenolase or diphenolase. The monophenolase form can be inactive or active. A huge amount of the active form is obtained in the presence of catechol (Dempsey et al., 2004). Catechol is oxidized to form *o*-quinone which is electrochemically reduced back to catechol. As it can be seen in Fig. 4, the cyclic voltammograms of catechol at the Tyr/SPE (curve a), Tyr/PASE–GO/SPE (curve b) and Tyr–Au/PASE–GO/SPE (curve c) in 0.1 M PBS (pH 7.0) containing 0.1 M KCl show obvious reduction peaks appearing at both of the electrodes, which is due to the reduction of enzymatic reaction product (*o*-quinone). The steps of the enzymatic reaction are shown as follows:

$$\text{catechol} + \text{tyrosinase}(O_2) \rightarrow o\text{-quinone} + H_2O \quad (1)$$

$$o\text{-quinone} + 2H + 2e^- \rightarrow \text{catechol} \quad (2)$$

At the Tyr/SPE, there was a pair of reversible redox peaks (curve a). In the case of Tyr/PASE–GO/SPE (curve b), the observed oxidation peak decreased; the reduction peak was heightened; and the potential shifted negatively, which was obviously attributed to the direct reduction of *o*-quinone liberated from the enzyme-catalyzed reaction on the electrode surface. This may due to the following two reasons. Firstly, the presence of GO sheets in the nanocomposite results in the improvement of electron transfer kinetic and

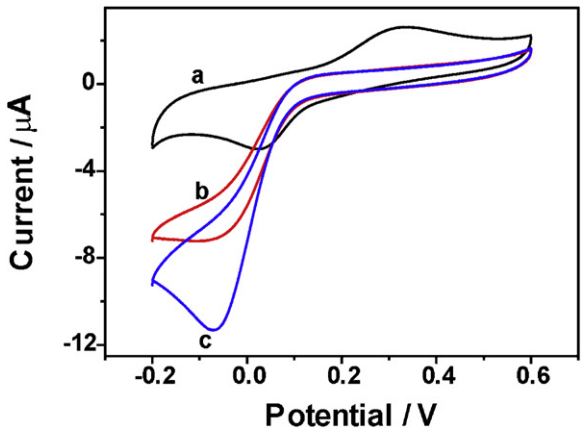

Fig. 4. Cyclic voltammograms of 1.0×10^{-4} M catechol in 0.1 M PBS (pH 7.0) at Tyr/SPE (a); Tyr/PASE–GO/SPE (b); and Tyr–Au/PASE–GO/SPE (c).

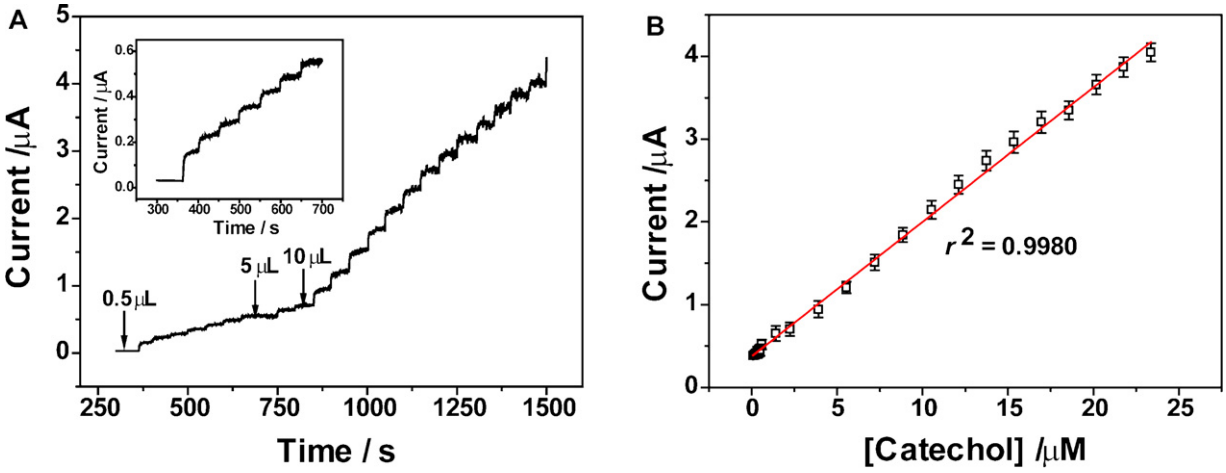

Fig. 5. (A) Typical current-time response curves for the successive addition of 1 mM catechol in 0.1 M PBS (pH 7.0) on Tyr–Au/PASE–GO/SPE at an applied potential of −0.2 V vs. Ag/AgCl. Inset: the magnification of initial steps; (B) Calibration curves for catechol obtained at Tyr–Au/PASE–GO/SPE.

enhancement in the reduction current of *o*-quinone, which may be ascribed to the high surface area and the unique electrical conductivity of the graphene nanosheets. Secondly, tyrosinase molecules covalently bind with the PASE–GO by forming the amide bond with PASE molecules, resulting in the increasement of enzyme loading. Comparing to the Tyr/SPE, more *o*-quinone molecules are liberated from the enzyme-catalyzed reaction on the Tyr/PASE–GO/SPE surface, leading to the larger reduction current.

Comparing the reduction peak currents of catechol at the Tyr/PASE–GO/SPE with the Tyr–Au/PASE–GO/SPE, the AuNPs in the nanocomposite dramatically enhanced the electrochemical response of catechol, resulting in an increasing reduction current. The tyrosinase could retain its bioactivity to a large extent by the covalently binding due to the unique properties of GO–Au complex and the synergistic effect (Zhou et al., 2010a). On one hand, the good biocompatibility of GO and AuNPs make the enzyme keep bioactivity well; On the other hand, GO and AuNPs can both provide more active sites for the electrode by their high specific surface area.

It is clear that the reduction peak current of catechol on the Tyr/PASE–GO/SPE depends linearly on the scan rate in the range from 20 to 120 mV s^{-1} (Figure S2 in supplementary materials), which is expected for a surface-controlled process.

3.4. Optimization of experimental parameters

To determine the optimum applied potential for the biosensor operation, amperometric measurements were carried out in 5.0 μM catechol. Figure S3A (in supplementary materials) displays the effect of the applied potential of the disposable biosensor on the amperometric response of catechol. The biosensor was operated at a different potential changing from −0.3 to 0.1 V (with 50 mV potential step), and the transient currents were permitted to attenuate to a steady-state value. As can be seen, the response of the biosensor increases with the change of applied potential from 0.1 to −0.3 V. The highest sensitivity is obtained at −0.25 V. The lower potential may bring interferences from other electro-active species. Therefore, the potential of −0.2 V was selected for the amperometric experiments.

The effect of pH value on the current response of the biosensor to 5.0 μM catechol in 0.1 M PBS was investigated with the pH range from 6.0 to 8.0, and the results are shown in Figure S3B (in supplementary materials). It can be seen that the response current increases with pH value ranging from 6.0 to 8.0, after reaching its maximum at pH 7.0, then it decreases as pH increases further. In order to achieve the maximum sensitivity, pH 7.0 PBS was selected as the electrolyte in subsequent experiments. This is in accordance with the optimum pH range in the reported literature (Xue and Shen, 2002).

3.5. Amperometric response of the biosensor

The amperometric response of the disposable biosensor of catechol was further evaluated under the optimized experimental conditions. As it can be seen in Fig. 5A, the fabricated Tyr–Au/PASE–GO/SPE biosensor shows a bioelectrocatalytic response rapidly and sensitively, reaching 95% of the steady-state current within 6 s after each addition of catechol, which means that small molecules have a rapid diffuse from the solution into the bionanocomposite film. Fig. 5B shows the typical calibration curve of the tyrosinase modified electrode to catechol. The biosensing performance is given as follows, linear response range (LRR) from 8.3×10^{-8} to 2.3×10^{-5} M with a linearity regression equation (LRE) of I (μA) = 0.16 C (μM) + 0.37 (r^2 = 0.9980), a limit of quantitation (LOQ) of 8.2×10^{-8} M (S/N = 10) and a limit of detection (LOD) of 2.4×10^{-8} M (S/N = 3). The Michaelis–Menten constant (K_{mapp}) is estimated to be 0.027 mM from the data obtained from the amperometric response, indicating that the immobilized tyrosinase strongly adsorbed on the surface of biosensor and increased affinity to catechol.

3.6. Reproducibility, stability, recovery and interference

The repeatability of the disposable biosensor was investigated by detecting 10 μM catechol for ten times successive determinations, with a relative standard deviation (RSD) value of 3.9%. This result shows the biosensor has a good repeatability without using a complicated pretreatment procedure to the SPE. The reproducibility was also examined with ten different SPEs constructed by the same step independently. The RSD was 5.1% for the response current to 10 μM catechol, demonstrating that the fabrication procedure was reliable and the modified SPE had good reproducibility.

The biosensor's storage stability was also evaluated by measuring its response to 10 μM catechol in 0.1 M PBS containing 0.1 M KCl (pH 7.0) at −0.2 V. The results show that the activity of the biosensor retained 89% of its original response after 20 days and then decreased gradually to about 54% after 2 months. The relatively good stability may explain the fact that this Tyr–Au/PASE–GO bionanocomposite film could provide a biocompatible

microenvironment to protect the specific ability of tyrosinase effectively.

The amperometric responses of the Tyr–Au/PASE–GO/SPE biosensor to other phenolic compounds were investigated. The biosensor has good responses to catechol, phenol, *p*-cresol and *p*-chlorophenol, and the sensitivity for these four compounds followed the general trend: catechol ($160\,mA\,M^{-1}$) > *p*-cresol ($153\,mA\,M^{-1}$) > *p*-chlorophenol ($142\,mA\,M^{-1}$) > phenol ($84\,mA\,M^{-1}$). This sequence for catechol, phenol, and *p*-cresol is the same as that reported in previous works (Kochana et al., 2008; Wang et al., 2008; Zhao et al., 2009). The sensitivities for other phenolic compounds (*o*-aminophenol, resorcinol and *p*-acetamidophenol) were less than $2\,mA\,M^{-1}$. The different sensitivity for different phenolic compounds may depend on the tyrosinase catalytic selectivity for different phenolic compounds.

The practical application of the biosensor was also tested by the catechol recovery experiments in water samples, with average recoveries from 94.2% to 104.7%, as presented in Table S1 (in supplementary materials). The satisfactory results confirmed that the disposable biosensor could be used for practical phenol detection.

The selectivity of the biosensor was investigated by detecting the response to 10 μM catechol in the presence of some possible interferents, with the following results: 10 mM K^+, Na^+, Cl^-, HPO_4^{2-}, $H_2PO_4^-$, Ac^-, NO_3^-, Cu^{2+}; 100 μM nitrobenzene, 1 mM ethanol, acetone, glucose does not show the significant interfering effect. Besides, nitrophenol, when present in a concentration of 10 μM, causes a slightly negative error.

4. Conclusion

In summary, we have developed a disposable tyrosinase biosensor based on the immobilization of tyrosinase-protected gold nanoparticles onto the 1-pyrenebutanoic acid, succinimidyl ester functional graphene oxide for the determination of catechol. The bifunctional molecule PASE was assembled onto GO sheets through noncovalent interaction, which was confirmed by UV–vis, FT-IR and AFM. Subsequently, the Tyr–Au was immobilized on the PASE–GO sheets forming a biocompatible nanocomposite. TEM indicated that Tyr–Au successfully assembled onto the functionalized GO sheets. The disposable tyrosinase biosensor was fabricated by modifying the screen printed electrode with the Tyr–Au/PASE–GO bionanocomposite. The biosensor provides a suitable microenvironment for retaining bioactivity of tyrosinase and exhibits a good analytical performance for the amperometric detection of catechol. In addition, this biosensor exhibits high sensitivity, good reproducibility and acceptable stability, showing a great potential for rapid, cost-effective and on-field analysis of phenolic compounds.

Acknowledgements

This work was supported by the National High Technology Research and Development Program of China (No. 2008AA06A406), the Fundamental Research Funds for the Central Universities (WK1013002), the Program for Professor of Special Appointment (Eastern Scholar) at Shanghai Institutions of Higher Learning, Ministry of Health (Grant 2009 ZX 10004-301), the Shanghai Postdoctoral Sustentation Fund of China (No. 09R21411700) and the Scientific Research Project of NCCT (No. NHKY-2010-05).

Appendix A. Supplementary data

Supplementary data associated with this article can be found, in the online version, at doi:10.1016/j.bios.2010.12.022.

References

Arecchi, A., Scampicchio, M., Drusch, S., Mannino, S., 2010. Anal. Chim. Acta 659, 133–136.
Bale, S., Asuri, P., Karajanagi, S., Dordick, J., Kane, R., 2007. Adv. Mater. 19, 3167–3170.
Chang, S.C., Rawson, K., McNeil, C.J., 2002. Biosens. Bioelectron. 17, 1015–1023.
Chen, D., Tang, L., Li, J., 2010. Chem. Soc. Rev. 39, 3157–3180.
Chen, R.J., Zhang, Y., Wang, D., Dai, H., 2001. J. Am. Chem. Soc. 123, 3838–3839.
Dempsey, E., Diamond, D., Collier, A., 2004. Biosens. Bioelectron. 20, 367–377.
Fang, Y., Guo, S., Zhu, C., Zhai, Y., Wang, E., 2010. Langmuir 26, 11277–11282.
Hong, W.J., Bai, H., Xu, Y.X., Yao, Z.Y., Gu, Z.Z., Shi, G.Q., 2010. J. Phys. Chem. C 114, 1822–1826.
Jaegfeldt, H., Kuwana, T., Johansson, G., 1983. J. Am. Chem. Soc. 105, 1805–1814.
Kampouris, D.K., Kadara, R.O., Jenkinson, N., Banks, C.E., 2009. Anal. Methods 1, 25–28.
Kochana, J., Gala, A., Parczewski, A., Adamski, J., 2008. Anal. Bioanal. Chem. 391, 1275–1281.
Kotte, H., Gruendig, B., Vorlop, K.-D., Strehlitz, B., Stottmeister, U., 1995. Anal. Chem. 67, 65–70.
Kovtyukhova, N.I., Ollivier, P.J., Martin, B.R., Mallouk, T.E., Chizhik, S.A., Buzaneva, E.V., Gorchinskiy, A.D., 1999. Chem. Mater. 11, 771–778.
Kurppa, K., Jiang, H., Szilvay, G., Nasibulin, A., Kauppinen, E., Linder, M., 2007. Angew. Chem. Int. Ed. 46, 6446–6449.
Li, F., Yang, H., Shan, C., Zhang, Q., Han, D., Ivaska, A., Niu, L., 2009. J. Mater. Chem. 19, 4022–4025.
Liu, Y., Yu, D., Zeng, C., Miao, Z., Dai, L., 2010. Langmuir 26, 6158–6160.
Liu, Z., Liu, Y., Yang, H., Yang, Y., Shen, G., Yu, R., 2005. Electroanalysis 17, 1065–1070.
Lu, J., Do, I., Drzal, L.T., Worden, R.M., Lee, I., 2008. ACS Nano 2, 1825–1832.
Mkhoyan, K.A., Contryman, A.W., Silcox, J., Stewart, D.A., Eda, G., Mattevi, C., Miller, S., Chhowalla, M., 2009. Nano Lett. 9, 1058–1063.
Montereali, M.R., Seta, L.D., Vastarella, W., Pilloton, R., 2010. J. Mol. Catal. B: Enzyme 64, 189–194.
Niyogi, S., Bekyarova, E., Itkis, M.E., McWilliams, J.L., Hamon, M.A., Haddon, R.C., 2006. J. Am. Chem. Soc. 128, 7720–7721.
Portaccio, M., Di Tuoro, D., Arduini, F., Lepore, M., Mita, D.G., Diano, N., Mita, L., Moscone, D., 2010. Biosens. Bioelectron. 25, 2003–2008.
Sapelnikova, S., Dock, E., Ruzgas, T., Emnéus, J., 2003. Talanta 61, 473–483.
Shan, C., Yang, H., Han, D., Zhang, Q., Ivaska, A., Niu, L., 2010. Biosens. Bioelectron. 25, 1070–1074.
Shan, D., Zhu, M., Han, E., Xue, H., Cosnier, S., 2007. Biosens. Bioelectron. 23, 648–654.
Shao, Y.Y., Wang, J., Wu, H., Liu, J., Aksay, I.A., Lin, Y.H., 2010. Electroanalysis 22, 1027–1036.
Solná, R., Dock, E., Christenson, A., Winther-Nielsen, M., Carlsson, C., Emnéus, J., Ruzgas, T., Skládal, P., 2005. Anal. Chim. Acta 528, 9–19.
Song, W., Zhang, L., Shi, L., Li, D.-W., Li, Y., Long, Y.-T., 2010. Microchim. Acta 169, 321–326.
Subrahmanyam, K.S., Ghosh, A., Gomathi, A., Govindaraj, A., Rao, C.N.R., 2009. Nanosci. Nanotechnol. Lett. 1, 28–31.
Sun, X., Liu, Z., Welsher, K., Robinson, J., Goodwin, A., Zaric, S., Dai, H., 2008. Nano Res. 1, 203–212.
Tan, Y., Deng, W., Ge, B., Xie, Q., Huang, J., Yao, S., 2009. Biosens. Bioelectron. 24, 2225–2231.
Tan, Y., Guo, X., Zhang, J., Kan, J., 2010. Biosens. Bioelectron. 25, 1681–1687.
Wang, H., Hao, Q., Yang, X., Lu, L., Wang, X., 2010. ACS Appl. Mater. Interfaces 2, 821–828.
Wang, S., Tan, Y., Zhao, D., Liu, G., 2008. Biosens. Bioelectron. 23, 1781–1787.
Wang, Z., Zhou, X., Zhang, J., Boey, F., Zhang, H., 2009. J. Phys. Chem. C 113, 14071–14075.
Wei, G., Pan, C., Reichert, J., Jandt, K.D., 2010. Carbon 48, 645–653.
Wu, Z.Q., 2008. J. Appl. Polym. Sci. 110, 777–783.
Xu, Y., Bai, H., Lu, G., Li, C., Shi, G., 2008. J. Am. Chem. Soc. 130, 5856–5857.
Xue, H., Shen, Z., 2002. Talanta 57, 289–295.
Yang, J., Pang, F.Y., Zhang, R.Y., Xu, Y., He, P.A., Fang, Y.Z., 2008. Electroanalysis 20, 2134–2140.
Zhang, J., Zhang, F., Yang, H., Huang, X., Liu, H., Zhang, J., Guo, S., 2010a. Langmuir 26, 6083–6085.
Zhang, X., Feng, Y., Tang, S., Feng, W., 2010b. Carbon 48, 211–216.
Zhao, J., Wu, D., Zhi, J., 2009. Bioelectrochemistry 75, 44–49.
Zhou, K., Zhu, Y., Yang, X., Li, C., 2010a. Electroanalysis 22, 259–264.
Zhou, Y., Liu, S., Jiang, H.J., Yang, H., Chen, H.Y., 2010b. Electroanalysis 22, 1323–1328.
Zuo, X., He, S., Li, D., Peng, C., Huang, Q., Song, S., Fan, C., 2010. Langmuir 26, 1936–1939.